

AD-A137 278

DETAILED KINETIC STUDIES OF EXCITED AND/OR TRANSIENT
SPECIES(U) UNIVERSITY OF SOUTHERN CALIFORNIA LOS
ANGELES C WITTIG JAN 84 N00014-82-K-0609

1/1

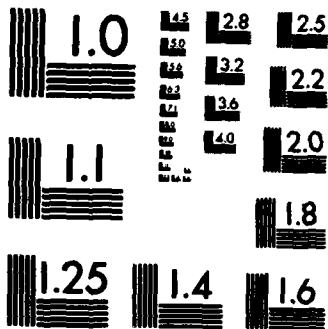
UNCLASSIFIED

F/G 20/5

NL



END
FILMED
DTIC



MICROCOPY RESOLUTION TEST CHART
NATIONAL BUREAU OF STANDARDS-1963-A

Unclassified

13

SECURITY CLASSIFICATION OF THIS PAGE (When Data Entered)

REPORT DOCUMENTATION PAGE

READ INSTRUCTIONS BEFORE COMPLETING FORM

1. REPORT NUMBER	2. GOVT ACCESSION NO.	3. RECIPIENT'S CATALOG NUMBER
4. TITLE (and Subtitle) Detailed Kinetic Studies of Excited and/or Transient Species		5. TYPE OF REPORT & PERIOD COVERED Final 6/1/82-5/31/83
7. AUTHOR(s) Curt Wittig		6. PERFORMING ORG. REPORT NUMBER
9. PERFORMING ORGANIZATION NAME AND ADDRESS University of Southern California University Park Los Angeles, CA 90089		8. CONTRACT OR GRANT NUMBER(s) N00014-82-K-0609
11. CONTROLLING OFFICE NAME AND ADDRESS Dr. Matt White Office of Naval Research 666 Summer Street, Bldg. 114, Section D Boston, MA 02210		10. PROGRAM ELEMENT, PROJECT, TASK AREA & WORK UNIT NUMBERS
14. MONITORING AGENCY NAME & ADDRESS (if different from Controlling Office)		12. REPORT DATE January 1984
		13. NUMBER OF PAGES 17
		15. SECURITY CLASS. (of this report) unclassified
		15a. DECLASSIFICATION/DOWNGRADING SCHEDULE

16. DISTRIBUTION STATEMENT (of this Report)

unlimited

17. DISTRIBUTION STATEMENT (of the abstract entered in Block 20, if different from Report)

unlimited

18. SUPPLEMENTARY NOTES

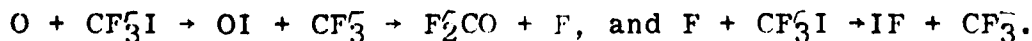
DTIC SELECTED
JAN 26 1984

19. KEY WORDS (Continue on reverse side if necessary and identify by block number)

kinetics, iodine monofluoride, laser induced fluorescence

20. ABSTRACT (Continue on reverse side if necessary and identify by block number)

Subsequent to the pulsed photolytic (193 nm) production of O(³P) in the presence of CF₃I, rapid consecutive reactions lead to the production of IF(X^{1,2}). All of our measurements are consistent with IF being produced via the reactions:



This route can be quite efficient, and we estimate that >10% of the O(³P) atoms can lead to IF molecules under suitable conditions.

AD A 137278

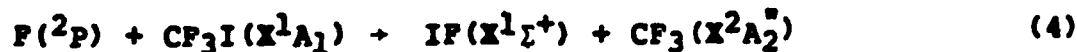
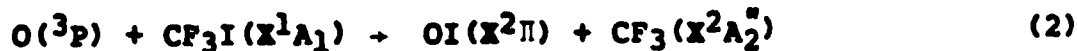
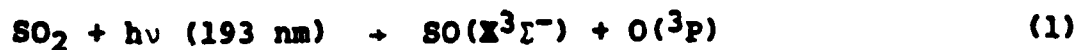
DTIC FILE COPY

I. INTRODUCTION

Iodine monofluoride, as well as the other diatomic interhalogens, has attracted attention as a candidate laser species which can be excited by chemical⁽¹⁻³⁾ and optical⁽³⁾ pumping methods, and has also been made to lase on ionic-covalent transitions in the blue-green portion of the spectrum (491 nm) using electron beam pumping and transverse electric discharges.⁽⁴⁻⁶⁾ Its physical and chemical properties are similar to those of the other interhalogens, and it has a substantial bond strength ($22,333 \text{ cm}^{-1}$), which does not allow for disproportionation into I_2 and F_2 .⁽⁷⁾ However, it is thermochemically and kinetically unstable, and it has only been observed in transient environments.⁽⁸⁾ Even though it has not been seen in absorption, it has been detected by emission spectroscopy^(2,9,10) and by laser induced fluorescence (LIF),^(7,11-13) and therefore it is possible to monitor quantum states of IF with excellent sensitivity and time resolution in the environments in which it is formed and removed.

Although a great deal is now understood about the properties of isolated IF molecules,^(7,10,12,14) there have been no reported instances in which the temporal of [IF] has been directly monitored (e.g. via LIF) in chemical systems. In this paper experimental results are presented which show how $\text{IF}(\text{X}^1\Sigma^+)$ is formed by reactions which occur subsequent to, and in parallel with, the reaction of atomic oxygen with CF_3I , following the

effectively instantaneous production of $O(^3P)$ in the presence of CF_3I :



where the enthalpy changes for reactions (3) and (4) are -80.9 and $-23.9 \text{ kcal mol}^{-1}$ respectively,⁽¹⁵⁾ and the enthalpy change for reaction (2) is quite uncertain.⁽¹⁶⁻¹⁹⁾ These processes produce IF in sufficient concentration that it can be detected very easily, and $IF(X^1\Sigma^+)$ can be made one of the major products by the proper choice of experimental parameters. Such processes can be important in environments wherein one wishes to maximize the production of excited species and minimize the production of ground state species (e.g. a laser device).

Accession For	
NTIS GRA&I	<input checked="" type="checkbox"/>
DTIC TAB	<input type="checkbox"/>
Unannounced	<input type="checkbox"/>
Justification	
By _____	
Distribution/	
Availability Codes	
Dist	Avail and/or Special
A-1	



II. EXPERIMENTAL

The experimental arrangement is shown schematically in Fig. 1. Atomic oxygen is prepared photolytically, on a time scale short compared to that of the subsequent events, by the excimer laser photolysis of SO_2 at 193 nm ($\sigma = 6 \times 10^{-18} \text{ cm}^2$).⁽²⁰⁾ Buffer gas insures that 300 K equilibration exists for the rotational and translational degrees of freedom, and that diffusion is minimized in our experiments. At this photolysis wavelength, CF_3I is photolyzed some ($\sigma \leq 10^{-19} \text{ cm}^2$) but this photolysis does not produce atomic fluorine,⁽²¹⁾ and thus is not detrimental to the experiments. We estimated the CF_3I photolysis cross section separately by photodissociating static CF_3I samples with known 193 nm fluences, and measuring the loss of CF_3I by IR spectrophotometry, under conditions wherein the main recombination process produces C_2F_6 . Under typical experimental conditions, < 0.5% of the CF_3I molecules are photolyzed, compared to ~ 15% of the SO_2 molecules. Gases are continuously flowed through the sample chamber, and pressures are recorded with a capacitance manometer.

Subsequent to the production of atomic oxygen in the presence of CF_3I , reactions ensue which result in the formation of atomic fluorine and $\text{IF}(X^1\Sigma^+)$, hereafter referred to as IF, in addition to other chemically distinct species. These reactions are discussed in detail in section IV. IF is detected by LIF via the $X^1\Sigma^+(v=0) \rightarrow B^3\Pi(O^+)(v=5)$ system in the 480 nm region,⁽⁷⁾ using a tunable dye laser (Quanta Ray), and LIF signals are

digitized and averaged until suitable signal to noise ratio (S/N) is obtained. The use of a Corning 3-69 cut-on filter serves to discriminate against scattered dye laser radiation. Detailed accounts of such measurements have been published elsewhere, and will not be repeated here.⁽²²⁾ An unsuccessful attempt was made to detect IO via LIF on the (2 + 0) band of the $A^2\Pi \leftarrow X^2\Pi$ system at 445 nm,⁽¹⁷⁾ indicating that the upper state predissociates. Atomic fluorine is detected via its reaction with H_2 , forming vibrationally excited HF, hereafter referred to as HF^\dagger . An IR detector (InSb, Spectronics, photovoltaic, 1.2 cm^2 , 77 K) is used to monitor the HF^\dagger , thereby allowing us to follow the fluorine atom production. Again, signals are averaged until suitable S/N is obtained, and detailed accounts of the experimental arrangement can be found elsewhere.⁽²³⁾

The time evolution of the IF concentration is obtained by delaying the dye laser pulse with respect to the 193 nm pulse. For these measurements to be meaningful, it is necessary that the IF quantum state distribution not evolve in time because of vibrational and/or rotational (V,R) energy transfer. We therefore operated under experimental conditions wherein the V,R degrees of freedom are in equilibrium at 300 K (e.g. with suitable concentrations of N_2 buffer). This is easily verified by taking LIF spectra at different delay times. The spontaneous emission lifetime of the $B^3\Pi(O^+)$ state is sufficiently short ($\sim 8 \mu\text{s}$), that quenching of this state by species whose concentrations evolve in time during an experiment is unimportant.⁽⁷⁾ The 193 nm fluence was kept low ($10\text{-}20 \text{ mJ cm}^{-2}$)

in order to avoid sequential absorptions, which can be a problem in experiments of this nature,⁽²⁴⁾ and the dye laser radiation was maintained at fluences such that the LIF spectra reflect the unsaturated absorption spectrum. In several experiments, it was desirable to produce fluorine atoms photolytically in order to monitor their reactions in the absence of atomic oxygen. This was done by photolyzing XeF₂, which has a small, but for our purposes adequate, absorption cross section at 193 nm.⁽²⁵⁾

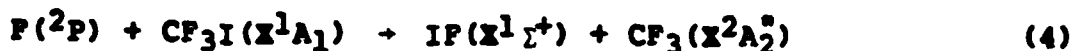
CF₃I (PCR, 97-99%) was distilled under vacuum and subjected to freeze-pump-thaw cycles prior to use in order to remove I₂ and C₂F₆ respectively. SO₂ (Matheson, 99.98%) was subjected to freeze-pump-thaw cycles prior to use, and XeF₂ (PCR, 99%), N₂ (Airco, 99.995%), and H₂ (Airco, 99.999%) were used without purification.

III. RESULTS

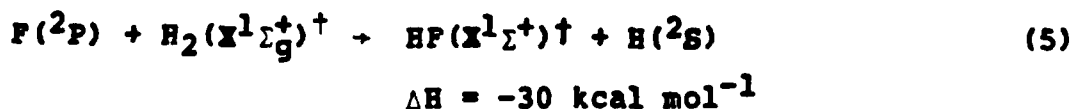
With samples containing CF_3I , either with or without N_2 buffer, but without a source of $O(^3P)$, the amount of IF produced was insignificant throughout the pressure range of the present study. For IF to be observed at all under those conditions, it was necessary to focus the excimer laser radiation and use CF_3I pressures of about 1 Torr. The requirement that the laser output be focused, and the prompt appearance of the IF, suggest that multiphoton absorption leads to IF under these conditions. When oxygen atoms are produced, however, large IF signals are obtained, and a typical LIF spectrum is shown in Fig. 2. We find that SO_2 is a convenient source of atomic oxygen because of the high photolysis efficiency at 193 nm. However, N_2O produces the same results, albeit with smaller signal intensities.

There is an obvious induction period for the production of IF at low $[CF_3I]$. This can be easily seen by detecting IF via LIF (see Fig. 3) with the laser frequency tuned to the bandhead frequency, under conditions wherein the V,R degrees of freedom are equilibrated at 300 K. At higher $[CF_3I]$, the induction period persists, but is not immediately evident to the untrained eye (Fig. 3c). For example, data such as those shown in Fig. 3, particularly at the higher $[CF_3I]$, can be "ascribed" a pseudo-first-order rate coefficient of $\sim 2 \times 10^{-12} \text{ cm}^3 \text{ molec}^{-1} \text{ s}^{-1}$ for the production of IF.

Under all of the conditions reported here, the reaction of F with CF₃I:



is rapid on the time scale of the measurements ($k_4 = 1.5 \times 10^{-10}$ cm³ molec⁻¹ s⁻¹), (26,27) and is not rate determining. This was checked separately, by photolyzing XeF₂ at 193 nm in the presence of CF₃I and N₂ buffer, and detecting the rapid appearance of IF via reaction (4). Thus, the production of IF reflects the production of F(^2P) in all of our experiments. If fluorine atoms are produced by reactions involving oxygen atoms, then it should also be possible to detect their presence by the well known reaction:



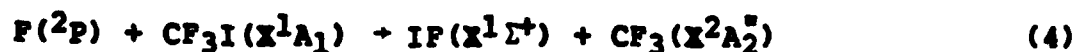
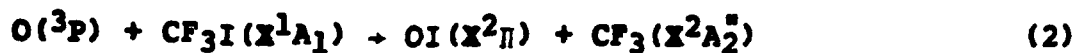
where $k_5 = 2.7 \times 10^{-11}$ cm³ molec⁻¹ s⁻¹. (28) Using a sensitive InSb IR detector, we monitored HF[†] emission following the production of O(^3P) via 193 nm photolysis. As in the case of the LIF detection of IF, there was no significant production of F(^2P) without first producing O(^3P). With sufficiently high [H₂], reaction (5) consumes fluorine atoms as fast as they are produced, and the rise of the HF[†] chemiluminescence signal reflects the rate of production of atomic fluorine. As with the IF LIF measurements, the HF[†] chemiluminescence signals can be

"ascribed" a pseudo-first-order rate coefficient, which in this case leads to $\sim 4 \times 10^{-12} \text{ cm}^3 \text{ molec}^{-1} \text{ s}^{-1}$. The reaction of $\text{O}(^3\text{P})$ with H_2 is negligibly slow at room temperature,⁽²⁹⁾ and does not affect the measurement.

The dependence of the IF LIF signal intensity on 193 nm laser fluence is shown in Fig. 4. These data are fit well by a quadratic fluence dependence (dashed curve), which is what is predicted by the proposed mechanism (see the Appendix).

IV. DISCUSSION

The only mechanism for the production of IF which is consistent with all of our measurements involves the following reactions:



Following 193 nm photolysis, $\text{O}(^3\text{P})$ is consumed rapidly by the large $[\text{CF}_3\text{I}]$, and reaction (3) proceeds by virtue of the CF_3 which is generated by reaction (2) as well as a small contribution from the 193 nm photolysis of CF_3I . The fluorine atoms thus produced react with CF_3I via reaction (4), thereby producing IF. Reactions (2) (19) and (4) (26,27,30) are well established, and reaction (3) has its parallel in the reaction:



which plays an important role in combustion ($k_6 = 1 \times 10^{-10} \text{ cm}^3 \text{ molec}^{-1} \text{ s}^{-1}$). (31) Thus, there are no surprises concerning the elementary processes which transpire to produce IF in this environment.

Although it was not our intention in this work to estimate rate coefficients for the different reactions, it is instructive to peruse the time development of the different concentrations of concern. The solution of the rate equations associated with

reactions (2) - (4) is given in the Appendix, and several pertinent points are discussed here. First, the apparent induction period, evident in Fig. 3, is seen to derive from the sequence of reactions leading to IF production. The dashed curves shown in Fig. 3 were computed using Eq. (A-5) for the time behavior of [IF], and the agreement is good. By monitoring fluorine atom production from reaction (3), via the HF^\dagger IR fluorescence, as well as IF production from reaction (4) via LIF, we were able to show that IF follows closely the production of atomic fluorine, as predicted by the proposed mechanism. Since there is no simple connection between the time evolution of [IF] and/or $[\text{HF}^\dagger]$, and genuine pseudo-first-order kinetics, the "apparent pseudo-first-order" behavior observed in the measurements is fortuitous and is not easily related to the rate coefficients for reactions (2) - (4). In fact, the $[\text{HF}^\dagger](t)$ and $[\text{IF}](t)$ signals yield rates of production which cannot be described by a single parameter τ_{rise} , and if the data are forced to fit a single exponential, the "apparent rate coefficient" is invariably smaller than k_2 , k_3 , or k_4 . Again, this is due to the sequential nature of the reactions which produce F and IF. In using Eq. (A-5), we are able to fit our measurements with a very reasonable estimate of k_3 .⁽³¹⁾ Since Eq. (A-5) was derived without allowing for the CF_3 which is produced directly by the 193 nm photolysis of CF_3I , an estimate of k_2 can be obtained by plotting the value of k_2 obtained from Eq. (A-5) vs. $[\text{CF}_3\text{I}]$, at constant 193 nm fluence, and extrapolating to $[\text{CF}_3\text{I}]=0$. The result of such a maneuver is shown in Fig. 5, and from this we

find that $k_2 = (6-7) \times 10^{-12} \text{ cm}^3 \text{ molec}^{-1} \text{ s}^{-1}$. This is about 40% lower than the literature value.⁽¹⁹⁾ We cannot account for this discrepancy, but such differences are not unknown in chemical kinetics. Thus, the efficient production of IF following the photolytic production of atomic oxygen in the presence of CF_3I is a consequence of sequential reactions involving radical intermediates, and a significant fraction of $[\text{O}]_0$ can be converted to [IF] in this manner.

ACKNOWLEDGEMENTS

The authors acknowledge useful discussions with H. Reisler, F. Shokoohi, J. Caballero, Y. Haas, S. Henegan, and S. Benson, and the expert technical assistance of H. Lloyd, E. Dietl, and J. Emerson.

APPENDIX

Following the discussion in the text, the reactions of concern are:



and the associated rate equations for the species pertinent to the present discussion are:

$$\dot{[\text{O}]} = -(k_2[\text{CF}_3\text{I}] + k_3[\text{CF}_3]) [\text{O}] \quad (\text{A-1})$$

$$\dot{[\text{F}]} = k_3[\text{O}][\text{CF}_3] - k_4[\text{F}][\text{CF}_3\text{I}] \quad (\text{A-2})$$

$$\dot{[\text{CF}_3]} = k_2[\text{O}][\text{CF}_3\text{I}] + k_4[\text{F}][\text{CF}_3\text{I}] - k_3[\text{O}][\text{CF}_3] \quad (\text{A-3})$$

$$\dot{[\text{IF}]} = k_4[\text{F}][\text{CF}_3\text{I}] \quad (\text{A-4})$$

For the cases most germane to our experiments (e.g. $[\text{CF}_3\text{I}] \gg [\text{O}], [\text{CF}_3]$), $[\text{O}] = [\text{O}]_0 e^{-t/\tau_2}$, where $[\text{O}]_0$ is the $\text{O}(^3\text{P})$ concentration produced by 193 nm photolysis, and $\tau_2^{-1} = k_2[\text{CF}_3\text{I}]$. Since $[\text{F}]$ is removed as rapidly as it is formed, the steady state approximation to Eq. (A-2) can be used, yielding $[\text{F}] = k_3[\text{O}][\text{CF}_3]/k_4[\text{CF}_3\text{I}]$. Thus, Eq. (A-3) has the trivial solution $[\text{CF}_3] = [\text{O}]_0(1 - e^{-t/\tau_2})$ and the expression for $[\text{IF}](t)$ follows directly:

$$\begin{aligned}
 \dot{[IF]} &= k_4[F][CF_3I] = k_3[O][CF_3] \\
 &= k_3[O]_0^2 (e^{-t/\tau_2})(1-e^{-t/\tau_2})
 \end{aligned}$$

$$[IF](t) = \frac{k_3[O]_0^2}{2k_2[CF_3I]} \times (1-e^{-t/\tau_2})^2 \quad (A-5)$$

Note that the temporal behaviors of [IF] and [F] are the same, and that the desired induction period and fluence dependence are manifest in Eq. (A-5) (see Figs. 3 and 4). The above expressions are for cases where $[CF_3I] \gg [O], [CF_3]$, and inspection of Eq. (A-5) suggests conditions wherein [IF] can be made a large fraction (> 0.1) of $[O]_0$ at $t \gg \tau_2$ (e.g. $[O]_0 \sim [CF_3I]$). In the event that CF_3 is also produced by 193 nm photolysis, rate coefficients can be obtained by fitting Eq. (A-5) for different values of $[CF_3]_0$, and extrapolating to $[CF_3]_0 = 0$.

REFERENCES

1. R.D. Coombe and R.K. Horne, *J. Phys. Chem.* **83**, 2435 (1979).
2. M.A.A. Clyne, J.A. Coxon, and L.W. Townsend, *J.C.S. Faraday II* **68**, 2134 (1974).
3. S.J. Davis and L. Hanko, *Appl. Phys. Lett.* **37**, 692 (1980).
4. M. Diegelmann, H.P. Grieneisen, K. Hohla, K.L. Kompa, and J. Krasinsiki, *Laser Focus*, March 1980, pp. 50-52.
5. M. Diegelmann, K. Hohla, F. Rebentrost, and K.L. Kompa, *J. Chem. Phys.* **76**, 1233 (1982).
6. M. Diegelmann, H.P. Grieneisen, K. Hohla, Xue-Jing Hu, J. Krasinsiki, and K.L. Kompa, *Appl. Phys.* **23**, 283 (1980).
7. M.A.A. Clyne and I.S. McDermid, *J.C.S. Faraday II* **74**, 1644 (1978).
8. J.W. Birks, S.D. Gabelnick, and H.S. Johnston, *J. Mol. Spectr.* **57**, 23 (1975).
9. R.A. Durie, *Proc. Roy. Soc. (London), Ser. A* **207**, 388 (1951).
10. R.A. Durie, *Can. J. Phys.* **44**, 337 (1966).
11. M.A.A. Clyne and I.S. McDermid, *J.C.S. Faraday II* **72**, 2252 (1976).
12. M.A.A. Clyne and I.S. McDermid, *J.C.S. Faraday II* **73**, 1094 (1977).
13. R.J. Donovan, D.P. Fernie, M.A.D. Fluendy, R.M. Glen, A.G.A. Rae, and J.R. Wheeler, *Chem. Phys. Lett.* **69**, 472 (1980).
14. K.P.R. Nair, J. Hoefl, and E. Tiemann, *Chem. Phys. Lett.* **60**, 253 (1979).
15. D.R. Stull and H. Prophet, Project Directors, "JANAF Thermochemical Tables," 2nd ed., Natl. Stand. Ref. Data Ser-Nat. Bur. Stand. (U.S.) **9** (1967).
16. R.A. Durie and D.A. Ramsay, *Can. J. Phys.* **36**, 35 (1958).
17. R.A. Durie, F. Legay, and D.A. Ramsay, *Can. J. Phys.* **38**, 444 (1960).
18. M.A.A. Clyne and H.W. Cruse, *J.C.S. Faraday II* **66**, 2227 (1970).

19. M.C. Addison, R.J. Donovan, and J. Garraway, *J.C.S. Faraday II* 75, 286 (1979).
20. D. Golomb, K. Watanabe, and F.F. Marmo, *J. Chem. Phys.* 36, 958 (1962).
21. T. Donohue and J.R. Wiesenfeld, *J. Chem. Phys.* 63, 3130 (1975).
22. H. Reisler, M. Mangir, and C. Wittig, *J. Chem. Phys.* 71, 2109 (1979).
23. A. Hariri and C. Wittig, *J. Chem. Phys.* 67, 4454 (1977).
24. D.S.Y. Hsu and M.C. Lin, *Int. J. Chem. Kinet.* 10, 839 (1978).
25. M.B. Robin, "Higher Excited States of Polyatomic Molecules," Vol. 2, Academic Press, New York (1974).
26. J. W. Bozzelli and M. Kaufman, *J. Phys. Chem.* 77, 1748 (1973).
27. V.L. Tal'rose, B.V. Kudrov, I.O. Leipunskii, I.I. Morozov, and M.N. Larichev, *J. Chem. Phys.* 60, 4870 (1974).
28. D.J. Smith, D.W. Setser, K.C. Kim, and D.J. Bogan, *J. Phys. Chem.* 81, 901 (1977).
29. G.C. Light and J.H. Matsumoto, *Int. J. Chem. Kinet.* 12, 451 (1980).
30. M.E. Jacox, *Chem. Phys.* 51, 69 (1980).
31. N. Washida and K.D. Bayes, *Int. J. Chem. Kinet.* 8, 777 (1976).

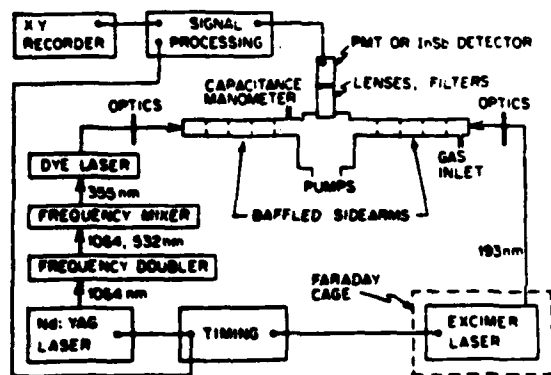


Fig. 1. Schematic drawing of the experimental arrangement.

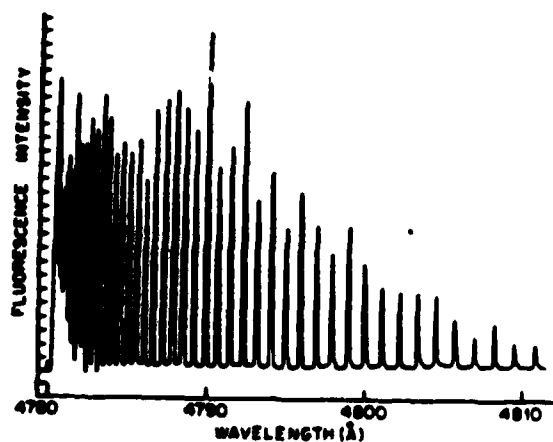


Fig. 2. LIF excitation spectrum of the $X \rightarrow B$ system of IF in the 480 nm region ($v' = 5 \rightarrow v'' = 0$). The spectrum was obtained with 50 mTorr SO_2 , 850 mTorr CF_3I , and 9.1 Torr N_2 . The probe dye-laser delay time was fixed at 100 μs . The dye-laser intensity was monitored continuously and was essentially constant throughout the measurement. The fluorescence was first passed through a Corning 3-69 cut-on filter which blocked all scattered laser light. Fluorescence signals were averaged until suitable S/N was achieved, typically 16 or 32 laser firings.

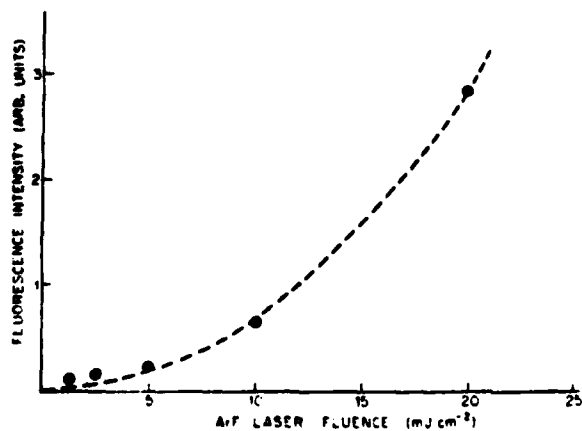


Fig. 4. IF LIF signal intensity versus ArF laser fluence. Each data point represents an average of 64 laser firings. The dashed curve represents a quadratic fluence dependence, as predicted by eq. (A.5). The conditions were: 5R mTorr SO_2 , 637 mTorr CF_3I , 9.3 Torr N_2 , 250 μs delay between the ArF and dye lasers.

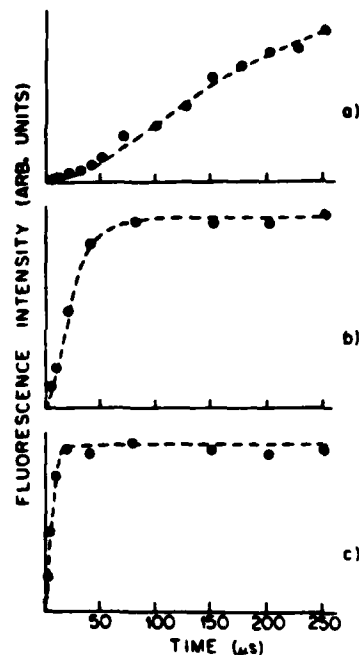


Fig. 3. IF LIF signal intensity versus the delay time between the ArF and dye lasers. The circles represent the data points averaged over 64 laser firings. The dashed curves are calculated from eq. (A.5). The gas mixes and values of k_2 used to fit the data were: (a) 2 mTorr SO_2 , 44 mTorr CF_3I , 9.95 Torr N_2 , $k_2 = 5.5 \times 10^{-12} \text{ cm}^3 \text{ molecule}^{-1} \text{ s}^{-1}$; (b) 59 mTorr SO_2 , 640 mTorr CF_3I , 9.3 Torr N_2 , $k_2 = 3.0 \times 10^{-12} \text{ cm}^3 \text{ molecule}^{-1} \text{ s}^{-1}$; (c) 68 mTorr SO_2 , 3.1 Torr CF_3I , 6.8 Torr N_2 , $k_2 = 2.5 \times 10^{-12} \text{ cm}^3 \text{ molecule}^{-1} \text{ s}^{-1}$. The value of k_2 obtained by extrapolating k_2 versus $[\text{CF}_3\text{I}]$ to $[\text{CF}_3\text{I}] = 0$ is $(6.5 \pm 1.5) \times 10^{-12} \text{ cm}^3 \text{ molecule}^{-1} \text{ s}^{-1}$ (see fig. 5). The time scale is chosen to illustrate the obvious induction period for production of IF at low $[\text{CF}_3\text{I}]$ (a) and the onset of apparent pseudo-first-order kinetics at higher $[\text{CF}_3\text{I}]$ (b) and (c) in which the data can be fitted (or nearly fitted) to a single exponential rise when the induction period is hidden by an inappropriate time scale.

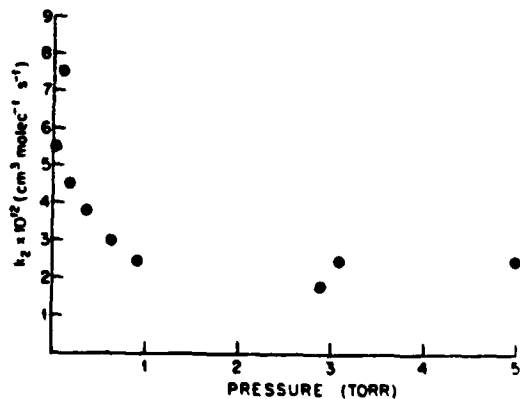


Fig. 5. k_2 , calculated from eq. (A.5) versus the pressure of CF_3I . See discussion in text.

END

FILMED

02 - 84

DTIC